Archives available at journals.mriindia.com

International Journal of Advanced Electrical and Electronics Engineering

ISSN: 2278-8948

Volume 13 Issue 01, 2024

A Bench Demonstrator for Inductive Roadway Power Transfer And 433 MHz In-Cabin Road-Signal Display

[1]Alex Pandian S, [2]Velmurugan M, [3]Bijo Johnson, [4]Jacob Thampi Vaidyan, [5]Jasmine J

[1,2,3,4,5]Department of Electrical and Electronics Engineering, Stella Mary's College of Engineering, Aruthenganvilai, Kanyakumari District, Tamil Nadu 629202, India

Peer Review Information

Submission: 19 Feb 2024
Revision: 15 March 2024
Acceptance: 14 April 2024

Keywords

Inductive Power Transfer, Dynamic Wireless Charging, Coupling Coefficient, Resonant Compensation, Quality Factor, Dwell Time, Energy per Pass, 433 MHz Telemetry, Vehicle-to-Infrastructure, Photovoltaic Supply, Measurement Integrity.

Abstract

This paper reports a bench demonstrator that combines two functions proposed for future road infrastructure: inductive power transfer to a moving vehicle from a renewably supplied roadway coil, and in-cabin display of road-signal information carried over a 433 MHz radio link. The demonstrator was built around an Arduino controller, a 433 MHz transmitter and receiver pair, a relay stage, coupled coils, a bridge rectifier, a DC-DC chopper, a linear regulator, a lead-acid battery and a 12 V 10 W photovoltaic panel. Its signalling function was shown to operate end to end. Its power-transfer chain was assembled and energised but never characterised, and the paper states this rather than substituting figures drawn from the literature. The principal contribution is therefore a disciplined separation of what this hardware measured from what the project record merely reproduced. The comparison table in that record, listing air gaps of 102 and 125 mm, operating frequencies of 20 and 22-23 kHz, link powers of 3.3 and 20 kW and efficiencies of 90 %, is reclassified here as reference data. The reclassification is arithmetic rather than cautionary: the quoted 20 kW exceeds the prototype's source rating by a factor of two thousand, and the panel's whole daily yield of roughly 50 Wh would sustain a 20 kW link for about nine seconds. No link efficiency, coupling coefficient, transferred power or air-gap tolerance is claimed for the built hardware, because none was measured. The paper consolidates the coupling, quality-factor, efficiency and dwell-time relations that govern dynamic charging; adds a table of independently verifiable parameters from full-scale systems and from the SAE J2954 standard for comparison; and derives from the dwell-time relation both the energy delivered in a single pad pass (approximately 0.33 Wh at 60 km/h from a 20 kW link) and the fraction of road length that would have to be electrified to offset an assumed 150 Wh/km consumption. The latter result, which exceeds 100 % of the road surface for a 3.3 kW link, is the quantitative fact that determines whether discrete-pad dynamic charging is viable at all.

Nomenclature

Symbol	Meaning
L_1, L_2	Primary and secondary self-inductance (H)
M, k	Mutual inductance (H) and coupling coefficient (dimensionless)
Q_1, Q_2	Primary and secondary quality factors (dimensionless)

ω_0, f_0	Resonant angular frequency (rad/s) and frequency (Hz)
C_1, C_2	Compensation capacitances (F)
R_1, R_2	Equivalent series resistance of each coil at the operating frequency (Ω)
η_{max}	Maximum achievable link efficiency (%)
z, r_c	Coil separation, that is air gap, and coil radius (m)
P_{link}	Power transferred across the inductive link (W)
L_p, v	Effective pad length (m) and vehicle speed (m/s)
t_{dwell}, E_{pass}	Dwell time (s) and energy delivered per pad pass (Wh)
P_{pv}, E_{day}	Photovoltaic panel rating (W) and daily energy yield (Wh)
E_{km}, L_{pad}	Assumed vehicle consumption (Wh/km) and pad length required per kilometre (m)

Introduction

Two distinct proposals for future road infrastructure motivate this work. The first is dynamic inductive power transfer (IPT), in which coils embedded in the road surface energise a receiving coil under a moving vehicle, so that charging occurs during travel rather than at a stop [1], [2], [3]. The second is the direct broadcast of signal and hazard information into the vehicle cabin, so that the driver's awareness does not depend on an unobstructed line of sight to a signal head [5].

Both proposals are attractive, and both are, at the level of physics and radio engineering, straightforward to demonstrate on a bench. The difficulty is entirely one of scale. The purpose of this paper is to make that difficulty quantitative rather than to obscure it. A demonstrator was built comprising coupled coils fed from a renewably supplied battery, a rectifier and chopper on the receiving side, and a 433 MHz link carrying signal information to a cabin display. The signalling function operated. The power-transfer function was assembled but never characterised, and the paper says so explicitly instead of substituting reference figures from the literature.

1. Problem Statement

Reports of student and prototype IPT systems commonly include a comparison table of static and dynamic charging parameters taken from full-scale published systems, positioned in the document so that a reader may reasonably take those numbers as the prototype's own performance. The gap addressed here is not technical but epistemic. It is the separation of a measured result from a reference datum, and the quantitative demonstration, by simple arithmetic on the source rating, of why the two cannot be confused in this case.

2. Objectives

The specific objectives of the work are as follows:

- To assemble a bench demonstrator that combines an inductive power-transfer chain with a 433 MHz road-signal link, using a photovoltaic supply.
- To report exactly what the assembled hardware was observed to do, and to report nothing further.
- To reclassify the comparison table held in the project record as literature reference data, and to justify that reclassification arithmetically rather than by assertion.
- To consolidate the coupling, resonance, quality-factor and efficiency relations that govern any IPT link, so that the quantities a future measurement campaign must obtain are identified in advance.
- To develop the dwell-time relation numerically, and from it the pad coverage that dynamic roadway charging would require, since this is the constraint that governs the viability of the concept.
- To specify a measurement path that would convert the demonstrator into a characterised link.

3. Scope and Delimitation

The study covers the assembly of the demonstrator, the relations governing inductive transfer, the arithmetic of source sizing and dwell time, and the specification of the measurements that were not taken. It explicitly excludes any claim about the built link's coupling coefficient, quality factor, transferred power, efficiency, air-gap tolerance or misalignment tolerance, since none of these was measured. It also excludes electromagnetic-compatibility and human-exposure assessment, which a deployed system would require but a bench demonstrator at this scale cannot meaningfully address. Figures drawn from the literature are labelled as such at every point of use.

4. Contributions

1. Explicit reclassification of the project's comparison table as literature reference data, supported by a scale computation showing that it is incompatible with the

prototype's 10 W source by three orders of magnitude.
2. A transparent statement of what the demonstrator did establish, namely the RF signalling path, and of what it did not.
3. Consolidation of the coupling, quality-factor and efficiency relations that govern an IPT link, with the measurement each one implies.
4. A dwell-time analysis giving energy per pad pass as a function of vehicle speed and link power, which is the governing constraint on dynamic roadway charging.
5. A derived coverage relation, new to this revision, giving the length of electrified pad required per kilometre to offset an assumed vehicle consumption, and showing that a 3.3 kW link cannot meet it even at complete road coverage.
6. A table of independently verifiable parameters from full-scale systems and from the SAE J2954 standard, provided so that the reference figures in the project record can be compared against published values rather than accepted on trust.
7. A measurement plan that would convert the demonstrator into a characterised link.

The remainder of the paper is organised as follows. Section II reviews related work and sets out verified reference parameters. Section III develops the governing relations. Section IV describes the demonstrator and the method. Section V reports the results, the reclassification, the scale analysis and the coverage analysis. Section VI discusses them, Section VII states the limitations, and Section VIII gives the proposed architecture and measurement path. Sections IX and X give the conclusion and the future scope.

Related Work

The literature on inductive power transfer for transport is mature on the electromagnetic side and thin on the reporting side, in the sense that prototype reports frequently mix measured and reference quantities. Table 1 summarises the works on which the present study draws, together with the role each plays here.

Table 1. Representative Related Work and its Relation to This Study

Ref.	Year	Focus and scope	Method and validation	Relation to this work
[1]	2013	Inductive power transfer for transport applications	Analysis and experiment	Source of Eqs. (1) to (3) and of the coupling-limited view of the link
[2]	1978	Roadway-powered electric vehicle	Early field demonstration	Origin of the dynamic-charging concept
[3]	—	On-line electric vehicle programme	Full-scale deployment	Source of the class of reference parameters reproduced in Table IV
[4]	2013	Double-D coil pad geometry	Design and measurement	Geometry referenced in this build; basis of the misalignment-tolerance claim
[5]	2016	In-vehicle signal information	Human-factors and field study	Safety case and reliability requirement for the RF cabin display
[6]	—	Arduino platform	Vendor documentation	Control layer of the demonstrator
[7]	2020	SAE J2954 wireless power transfer standard	Standardisation, interoperability testing	Independent benchmark for power class, frequency band and ground clearance
[8]	2013	KAIST OLEV buses and trams	Public revenue service	Verified dynamic-charging parameters, Table II
[9], [10], [11]	2016-2024	ORNL static wireless charging demonstrations	Laboratory and vehicle demonstration	Verified static power and efficiency figures, Table II
[12], [13], [14]	2022-2025	Electrified road deployments and trials	Field deployment in public traffic	Evidence that practical systems use continuous track, Section V-F

Covic and Boys [1] give the standard treatment of IPT for transportation, including compensation topologies and the coupling-limited nature of the link, and establish the figure of merit used in Eq.

(3). Bolger, Kirsten and Ng [2] reported the early roadway-powered vehicle work from which the dynamic-charging concept descends. Budhia and colleagues [4] introduced and characterised the double-D pad referenced in the present build, showing how flux-path shaping extends tolerance to lateral misalignment, a benefit that must be measured for each geometry rather than assumed. On the vehicle-to-infrastructure side, the literature on in-cabin signal presentation [5] establishes both the safety case and the reliability requirement, since a display that shows a stale or incorrect signal state is worse than no display at all.

Because the present paper turns on the difference between a measured value and a quoted one, it is useful to state a small set of parameters that can be checked against primary sources. These are collected in Table 2. They are not measurements of this demonstrator either, but unlike the figures in the project record their provenance is identifiable.

Table 2. Independently Verifiable Parameters from Full-Scale and Standardised Systems

System or standard	Link power	Frequency / air gap	Reported efficiency	Source
KAIST OLEV bus and tram	100 kW	20 kHz / 170-200 mm	85 %	KAIST public statements [8]
ORNL demonstration, 2016	20 kW	not stated in release	90 %	ORNL news release [9]
ORNL demonstration, 2018	120 kW	6 in (152 mm)	97 %	ORNL news release [10]
ORNL polyphase, 2024	270 kW	4.75 in (121 mm)	greater than 95 %	ORNL news release [11]
SAE J2954 WPT1 / WPT2 / WPT3	3.7 / 7.7 / 11 kW	81.39-90 kHz / 100-250 mm	not a single figure; performance criteria in standard	SAE J2954 [7]
Electreon receivers (dynamic)	7 and 11 kW light duty; up to 25 kW heavy duty	in-road coils; gap not stated	not stated in release	Public project reporting [12]
Arena of the Future test track, Brescia	1 MW supplied to a 1050 m track	in-road coils	not stated in release	Public project reporting [13]

Values in Table II are published figures for full-scale systems and standards. They are given so that the reader can compare the project record against identifiable sources. No value in this table was measured on the hardware described in Section IV.

Two observations follow from Table 2 and bear directly on the present work. First, the modern standardised band for light-duty wireless charging is centred on 85 kHz, within 81.39 to 90 kHz [7], whereas the 20 kHz figure that appears in the project record belongs to the earlier roadway-powered generation typified by OLEV [8]. A prototype table that mixes the two implicitly mixes two design eras. Second, the specific combination of values in the project record, in particular 3.3 kW at 102 mm and 20 kW at 125 mm, could not be traced to a primary source during this work. The 20 kW and 90 % pair is numerically close to the ORNL 2016 demonstration [9], but numerical closeness is not provenance, and no attribution is claimed here. The honest position is that the origin of those figures is not established, which is itself a reason not to present them as results.

Governing Relations

1. Coupling

Two coils of self-inductance L_1 and L_2 sharing a mutual inductance M have a coupling coefficient

$$k = \frac{M}{\sqrt{L_1 L_2}}, \quad 0 \le k \le 1 \tag{1}$$

For coaxial coils, k falls steeply once the separation approaches the coil radius, which is why the air gap is the dominant design variable in roadway charging. Fig. 1 shows this decay for two illustrative coil radii, with reference air gaps marked. The curve is illustrative only; the coil geometry of the present demonstrator was not characterised, so no point on it describes this build.

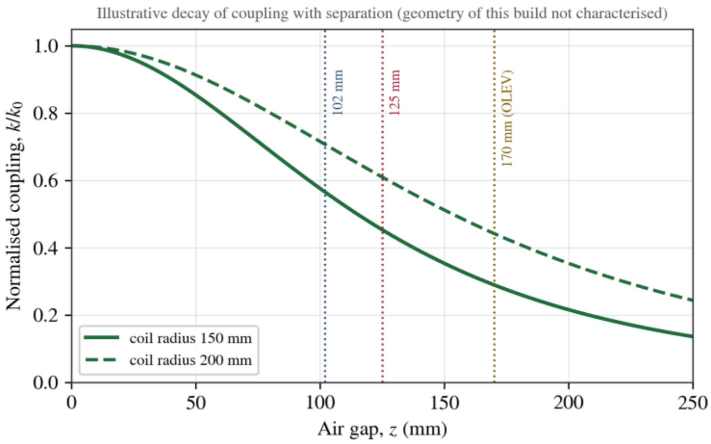

Figure 1: Illustrative decay of normalised coupling with air gap for two coil radii, with reference gaps marked. The geometry of this demonstrator was not measured.

2. Resonant Compensation and Quality Factor

Compensation capacitors tune each side to a common resonance, so that the reactive component of the coil impedance is cancelled and useful power can be transferred at modest coupling:

$$\omega_0 = \sqrt{\frac{1}{L_1 C_1}} = \sqrt{\frac{1}{L_2 C_2}}, \qquad Q_i = \frac{\omega_0 L_i}{R_i} \tag{2}$$

The quality factor Qi expresses how little energy each resonant tank dissipates per cycle. It rises with operating frequency and falls with coil resistance, which is why practical links use litz wire and low-loss compensation components.

3. Link Efficiency

The maximum efficiency achievable by an IPT link depends on k and Q only through their product [1]:

$$\eta_{\max} = \frac{k^2 Q_1 Q_2}{\left(1+\sqrt{1+k^2 Q_1 Q_2}\right)^2} \times 100\,\% \tag{3}$$

Equation (3) is plotted in Fig. 2. The practical consequence is important and often misstated in prototype reports. High efficiency at a large air gap is obtained not by improving coupling, which geometry bounds, but by raising the coil quality factor. This is why such links operate at tens of kilohertz with litz windings and high-Q compensation, and why a low-Q hand-wound coil pair cannot approach published efficiency figures however carefully it is aligned.

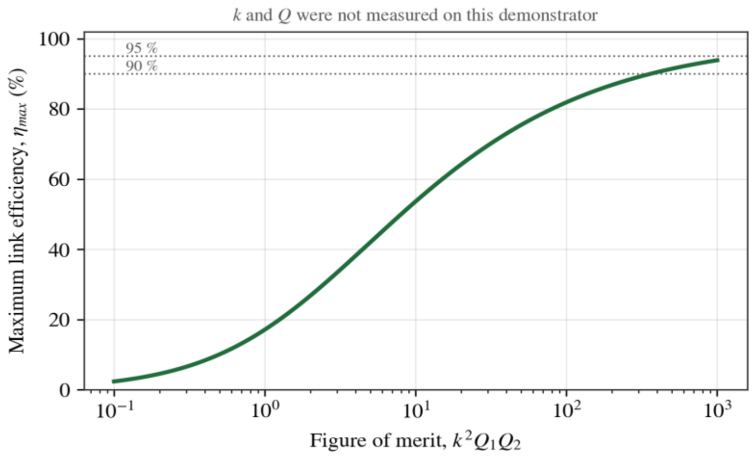

Figure 2: Maximum link efficiency against the figure of merit $k^2Q_1Q_2$ from Eq. (3). Neither k nor Q was measured on this demonstrator, so no point on this curve is attributable to it.

4. Dwell Time and Energy per Pass

The relation that governs dynamic charging is kinematic rather than electromagnetic. A vehicle at speed v crossing a pad of effective length L_p is coupled for

$$t_{\text{dwell}} = \frac{L_p}{v} \tag{4}$$

and receives, at link power P_{link},

$$E_{\text{pass}} = \frac{P_{\text{link}} L_p}{3600\, v} \quad [\text{Wh}] \tag{5}$$

Equation (5) is developed numerically in Section V-D, where it is shown to be the binding constraint on the entire concept.

Demonstrator and Methodology

1. Architecture

Fig. 3 shows the demonstrator. A 12 V 10 W photovoltaic panel charges a lead-acid battery, which supplies a switching stage driving the primary coil. The secondary coil feeds a bridge rectifier, a DC-DC chopper and a linear regulator to supply the receiving-side load. Independently of the power chain, an Arduino controller drives a 433 MHz transmitter representing the roadside signal state, and a matching receiver on the vehicle side drives an in-cabin indicator through a relay and transistor stage. The two wireless paths, shown dashed in the figure, are the inductive power link and the 433 MHz signalling link.

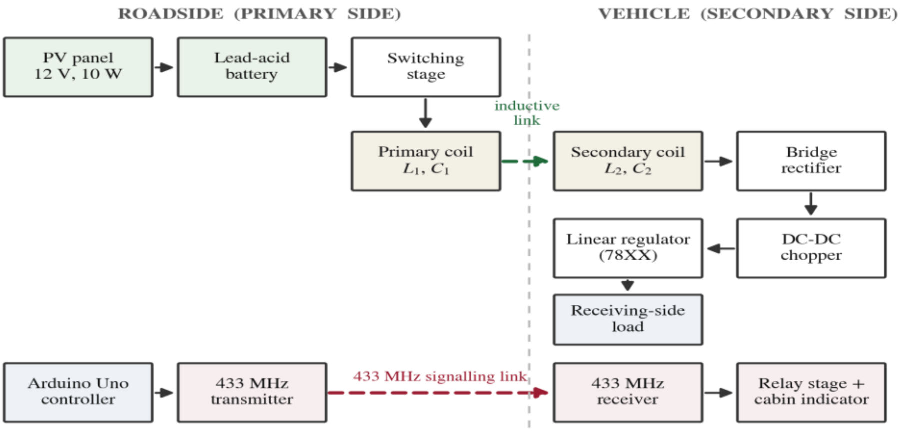

Figure 3: Demonstrator architecture. The dashed links are the two wireless paths: the inductive power link and the 433 MHz signalling link.

2. Apparatus

Table 3 lists the apparatus as documented in the project record. Ratings are given where the record states them, and are left blank where it does not.

Table 3. Demonstrator Apparatus as Documented

Item	Type / rating	Quantity
Photovoltaic panel	12 V, 10 W	1
Storage battery	Lead-acid	1
Controller board	Arduino Uno	1
RF transmitter and receiver	433 MHz pair	1 pair
Coupled coils	Circular pad / double-D	1 pair
Bridge rectifier	Full-wave	1
DC-DC chopper	Buck-boost	1
Linear regulator	78XX series	1
Relay module and transistors	Switching stage	1 set
Booster transformer	Rating not stated in the record	1

The switching frequency of the primary stage, the compensation capacitance values and the coil dimensions are not recorded. Their absence is the reason no operating point can be attributed to the built link.

3. Procedure

- Assemble the supply, switching, coil, rectification and regulation stages as shown in Fig. 3, and energise the chain from the photovoltaic-charged battery.
- Program the Arduino to transmit signal-state codes on the 433 MHz link.
- Confirm that the receiver reproduces the transmitted state and drives the cabin indicator through the relay stage.

4. What Was and What Was Not Instrumented

No impedance analyser, power analyser or synchronised two-sided voltage and current measurement was used at any point. No positional jig fixed or varied the air gap and the lateral offset. No spectrum measurement or packet-error count was taken on the radio link. The consequence is stated plainly, because it determines the whole of Section V: the demonstrator produced a functional observation on the signalling path and no quantitative observation at all on the power path.

Results

1. What the Demonstrator Established

The signalling path was shown to work end to end. A state asserted at the roadside transmitter was received and displayed on the vehicle-side indicator. The power chain was assembled and energised. That is the whole of the observed result, and it is reported here without extension.

2. Reclassifying the Comparison Table

The project record contains a table of static and dynamic charging parameters, reproduced here as Table 4. Its values are unchanged; its status is changed. These are published figures for full-scale systems of the kind described in [1] and [3], not measurements of this demonstrator. The reclassification is not a matter of caution but of arithmetic, as the next subsection shows.

Table 4. Parameters Reproduced from the Project Record (Not Measurements of This Demonstrator)

Mode	Gap (mm)	Frequency (kHz)	Power (kW)	Efficiency (%)	Time
Static	102	20	3.3 - 3.6	90	5 h
Dynamic	125	22 - 23	20	90	30 min

Values are reference data retained for context. No value in this table was measured on the hardware described in Section IV, and the primary source of this particular combination of values could not be identified during the present work.

3. The Scale Argument

The demonstrator's entire energy source is a 12 V 10 W photovoltaic panel. Comparing this with the power column of Table IV:

$$\frac{20\text{ kW}}{10\text{ W}} = 2000, \quad \frac{3.3\text{ kW}}{10\text{ W}} = 330 \tag{6}$$

The dynamic-charging entry exceeds the prototype's source rating by three orders of magnitude. Expressed as energy, and taking the panel to yield for five equivalent full-sun hours, which is an assumption and not a measurement,

$$E_{\text{day}} \approx 10\text{ W} \times 5\text{ h} = 50\text{ Wh} \tag{7}$$

which at 20 kW would sustain transfer for

$$t = \frac{50 \times 3600}{20000} = 9.0\text{ s} \tag{8}$$

in an entire day. No further argument is required. The table cannot describe this hardware, and treating it as a result would misstate the work by a factor of two thousand.

4. Dwell Time: The Binding Constraint

Equation (5) yields the quantity that determines whether dynamic roadway charging is worth building. Table 5 evaluates it for a one-metre effective pad at three speeds and three link powers, the last of these being the OLEV-class figure from Table II. Fig. 4 plots the same relation continuously.

Table 5. Dwell Time and Energy per Pad Pass for a 1 m Effective Pad (Computed from Eqs. (4) and (5))

Speed	Dwell time (s)	E_{pass} at 3.3 kW (Wh)	E_{pass} at 20 kW (Wh)	E_{pass} at 100 kW (Wh)
30 km/h	0.120	0.110	0.667	3.333
60 km/h	0.060	0.055	0.333	1.667
90 km/h	0.040	0.037	0.222	1.111

All entries are computed from the stated relations and the stated reference powers. None is a measurement of this demonstrator.

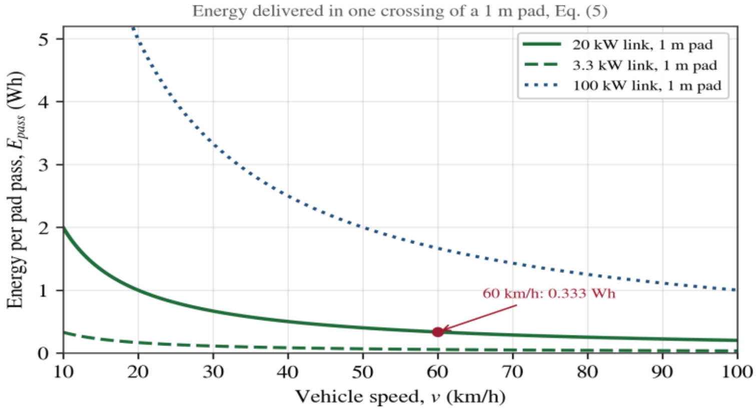

Figure 4: Energy delivered in a single crossing of a one-metre pad, from Eq. (5), for three link powers.

5. Required Pad Coverage

The dwell-time result becomes concrete when it is converted into the length of electrified pad a road would need. If a vehicle consumes E_{km} watt-hours per kilometre, then the pad length required per kilometre to offset that consumption follows directly from Eq. (5):

$$L_{\text{pad}} = \frac{3600\, E_{\text{km}}\, v}{P_{\text{link}}} \quad [\text{m per km}] \tag{9}$$

Table 6 evaluates Eq. (9) for an assumed consumption of 150 Wh/km, a figure typical of a light passenger electric vehicle and stated here as an assumption rather than a measurement. The result is expressed as the percentage of the road surface that would have to be pad. Fig. 5 plots the same quantity against speed.

Table 6. Percentage of Road Length That Must Be Electrified Pad, for an Assumed 150 Wh/km Consumption

Link power	at 30 km/h	at 60 km/h	at 90 km/h
3.3 kW	136 %	273 %	409 %
20 kW	22.5 %	45 %	67.5 %
100 kW	4.5 %	9 %	13.5 %

Computed from Eq. (9). A value above 100 % means the requirement cannot be met at any coverage: even a fully electrified road at that link power delivers less than the vehicle consumes. Perfect alignment and lossless transfer are assumed throughout, so these figures are optimistic bounds.

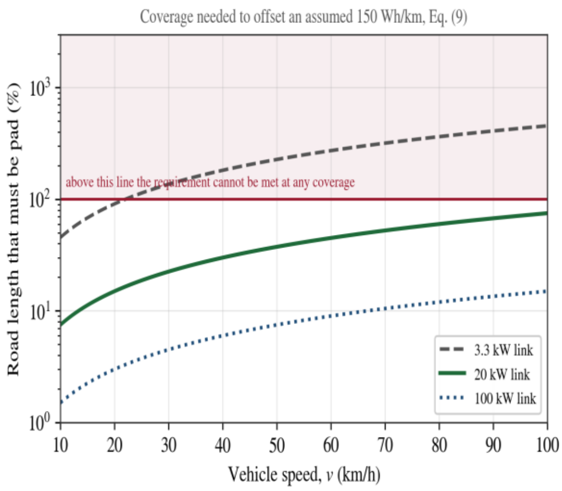

Figure 5: Road length that must be electrified pad, as a percentage, to offset an assumed consumption of 150 Wh/km. The horizontal line marks complete coverage, which is a physical ceiling.

Two consequences follow. A 3.3 kW link of the kind quoted in the project record cannot sustain highway-speed operation at any coverage, because at 60 km/h a fully electrified kilometre would deliver about 55 Wh against 150 Wh consumed. A 20 kW link requires roughly 45 % of the carriageway to be electrified at the same speed. Only at OLEV-class power does the requirement fall to a construction figure that could plausibly be built, and even then it applies to a single vehicle under ideal alignment.

6. Discrete Pads Compared with Continuous Track

The same arithmetic explains why field deployments do not use isolated pads. Fig. 6 compares the energy delivered in one traverse of a one-metre pad with that delivered over a 1050 m continuous track, the length used in the Arena of the Future installation at Brescia [13], at 60 km/h. The dwell time rises from 0.060 s to 63 s and the energy per traverse from 0.333 Wh to 350 Wh at 20 kW. The improvement is nothing more than the length ratio, which is precisely the point: in dynamic charging, delivered energy is bought with electrified metres, not with clever coil design.

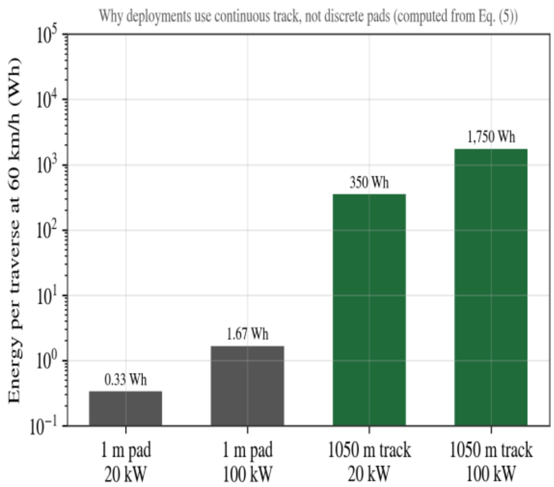

Figure 6: Energy per traverse at 60 km/h for a one-metre pad and for a 1050 m continuous track, computed from Eq. (5). The vertical axis is logarithmic.

7. What the Campaign Supports

Table 7 states the position quantity by quantity. It is the central table of the paper, and it is deliberately dominated by entries that were not obtained.

Table 7. Demonstrated, Documented, Reference and Indeterminate Quantities

Quantity or capability	Value	Status
RF signalling path functions	yes	demonstrated
Power chain assembled and energised	yes	demonstrated
Panel rating	12 V, 10 W	documented
Energy per 1 m pass at 60 km/h, 20 kW	0.33 Wh	computed, Eq. (5)
Pad coverage at 60 km/h, 20 kW	45 %	computed, Eq. (9)
Panel daily yield	approximately 50 Wh	computed from rating, Eq. (7)
Full-scale link efficiency	85 to 97 %	literature, Table II

Discussion

The demonstrator establishes one thing and clarifies another. It establishes that a 433 MHz link can carry roadside signal state to a cabin indicator with commodity components and an Arduino controller. It clarifies, through the arithmetic of Sections V-C to V-E, why the inductive half of the same concept cannot be evaluated on a bench supplied by a 10 W panel. These are different kinds of statement and the paper keeps them apart.

Table 8 sets out the qualitative properties that can be asserted, each with the relation or source that supports it. Nothing in the table depends on a measurement that was not made.

Table 8. Qualitative Properties and Their Basis

Feature	Property	Basis
IPT link	Efficiency is bounded by the product $k^2Q_1Q_2$	Eq. (3), after [1]
Air gap	Dominant variable; k falls steeply as separation approaches coil radius	Eq. (1)
Double-D geometry	Improves tolerance to lateral misalignment	[4]
Dynamic charging	Energy per pass falls as 1/v	Eq. (5)
Discrete pads	Coverage requirement scales with speed and inversely with link power	Eq. (9)
433 MHz link	Function demonstrated; range and reliability untested	This work
Cabin display	Requires fail-safe behaviour on loss of link	[5]
10 W photovoltaic source	Bounds any transfer demonstration to short bursts	Section V-C

1. The Signalling Function Requires its Own Metrics

The RF link worked, but a road-signal display is a safety-relevant function and its useful metrics were not collected. Range, packet loss under motion, the latency between a signal-head change and the cabin indication, and, most importantly, the behaviour on loss of reception were all untested. A display that retains a stale green indication after losing the link is more dangerous than no display at all, so fail-safe behaviour is a design requirement rather than a refinement, and it was not demonstrated here. The 433 MHz band is also unlicensed and shared, which makes interference and packet loss questions to be answered by measurement rather than assumptions to be made in a design note.

2. Notes on Unsupported Claims in the Source Material

Two further items in the project record are set aside. The design describes a hybrid solar and wind supply; no wind generation stage was built, and the demonstrator is solar only. The record also cites an annual figure for signal-violation fatalities without attribution. Unattributed statistics are not reproduced here, and any such figure should be taken from the official national road-accident statistics with the year and the counting definition stated alongside it.

Limitations

The following limitations bound every claim made in this paper.

- No electrical measurement of any kind was taken on the inductive link. Coupling coefficient, quality factor, transferred power, efficiency, air-gap tolerance and misalignment tolerance are therefore indeterminate for this build, not merely uncertain.
- The operating frequency, compensation capacitance and coil dimensions of the built stage are not recorded, so the

demonstrator cannot be reproduced from this paper alone.

- The signalling result is functional rather than quantitative. It shows that a state was conveyed, not how reliably, at what range or with what latency.
- The daily yield of 50 Wh assumes five equivalent full-sun hours. It is an assumption applied to a rating, not a measured generation figure.
- The consumption of 150 Wh/km used in Section V-E is an assumed representative value for a light passenger vehicle. Real consumption varies with mass, speed, gradient and auxiliary load.
- The coverage results of Table VI assume perfect alignment and lossless transfer, so they are optimistic bounds. Real coverage requirements would be higher.
- Figures 1 and 2 are illustrative plots of the governing relations. They contain no data point from this hardware.
- The parameters in Table IV are reference data of unestablished provenance. They are retained for context only and should not be cited from this paper as measurements of anything.

Proposed Architecture and Measurement Path

Fig. 7 shows what the demonstrator must acquire in order to become a characterised link: instrumentation on both sides of the coupling, a positional reference, and a fail-safe path on the signalling channel.

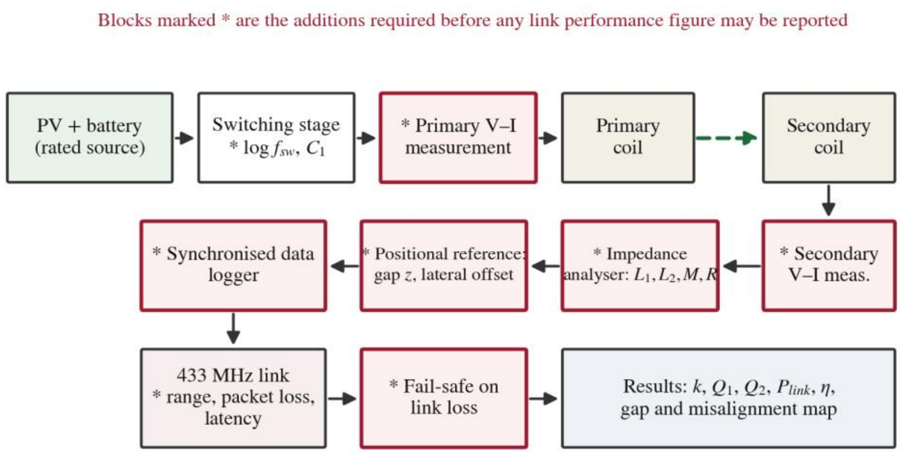

Figure 7: Proposed architecture. Blocks marked with an asterisk are the additions required before any link performance figure may be reported.

1. Characterising the Link

Measuring L_1, L_2 and M with an impedance analyser gives k directly through Eq. (1). Measuring coil resistance at the operating frequency gives Q through Eq. (2). Simultaneous voltage and current measurement on both sides gives P_{link} and the actual efficiency, which can then be compared against the bound of Eq. (3). Repeating the exercise across gap and lateral offset produces the efficiency map that any practical pad design requires [4]. Table 9 sets out the plan in full.

Table 9. Measurement Plan Required to Convert the Demonstrator into a Characterised Link

Measurement	Instrument or method	Quantity it yields
Self and mutual inductance	Impedance analyser or LCR bridge at the operating frequency	L_1, L_2, M and hence k, Eq. (1)
Coil series resistance	Impedance analyser at the operating frequency	R_1, R_2 and hence Q_1, Q_2, Eq. (2)
Two-sided power	Synchronised voltage and current logging on primary and secondary	P_{link} and true efficiency, compared against Eq. (3)
Gap and offset sweep	Positional jig with a repeatable reference datum	Efficiency map across z and lateral offset
Switching stage documentation	Oscilloscope and component measurement	Operating frequency and compensation values of the built stage

RF channel characterisation	Range trials with packet counting under motion	Range, packet-loss rate and state latency
Fail-safe verification	Deliberate link interruption during operation	Indicator behaviour on loss of reception
Source budget	Battery state-of-charge logging during a burst	Sustainable duration of any high-power demonstration

2. Sizing the Source Honestly

If a transfer demonstration at meaningful power is intended, the supply must be sized for it. A 10 W panel can charge a battery which then delivers a short high-power burst, and stating the burst duration alongside the power is the honest way to present such a demonstration. A claim of the form 'the link delivered P watts' should always be accompanied by 'for t seconds, from a source of E watt-hours', because the second clause is what distinguishes a transfer demonstration from a transfer capability.

Conclusion

A bench demonstrator combining an inductive power-transfer chain fed from a 12 V 10 W photovoltaic supply with a 433 MHz road-signal link was built. The signalling path was shown to work end to end. The power chain was assembled and energised but never characterised.

The project's comparison table, listing air gaps of 102 and 125 mm, frequencies of 20 and 22 to 23 kHz, powers of 3.3 and 20 kW and efficiencies of 90 %, was reclassified as literature reference data rather than measurement, and the reclassification was justified arithmetically: the quoted dynamic-charging power exceeds the demonstrator's source rating by a factor of two thousand, and the panel's entire daily yield of about 50 Wh would sustain such a link for roughly nine seconds. Accordingly no coupling coefficient, quality factor, transferred power, link efficiency or air-gap tolerance is claimed for the built hardware.

The coupling, resonance and efficiency relations governing such links were consolidated, and the dwell-time relation was developed numerically to show that a vehicle crossing a one-metre pad at 60 km/h receives about 0.33 Wh even from a 20 kW link. Extending that relation to a coverage requirement showed that offsetting an assumed 150 Wh/km at 60 km/h would need roughly 45 % of the carriageway to be electrified at 20 kW, and more than the whole carriageway at 3.3 kW. This is the constraint that dominates the viability of discrete-pad dynamic roadway charging, and it is consistent with the continuous-track geometry adopted in field deployments.

The signalling function was noted to require its own untested metrics, of which fail-safe behaviour on loss of reception is the most important. A measurement path was specified that would convert the demonstrator into a characterised link. The contribution of the paper is not a performance figure but a method of reporting: every number here is measured, computed with the computation shown, or labelled as literature or assumption.

Future Work

Several extensions follow directly from the limitations above.

- Measure the coupling-Determine L_1, L_2, M and coil resistance so that k, Q and the efficiency bound become results rather than symbols.
- Instrument both sides-Log primary and secondary voltage and current simultaneously to obtain transferred power and true efficiency.
- Map gap and misalignment-Repeat the measurement across separation and lateral offset to produce the tolerance map that a pad design requires.
- Document the operating frequency-Record the actual switching frequency and compensation values of the built stage, and compare them against the 81.39 to 90 kHz band standardised for light-duty wireless charging [7].
- Characterise the RF channel-Measure range, packet loss under motion and state latency, and implement and test fail-safe behaviour on link loss.
- State the source budget-Present any high-power demonstration together with its sustainable duration from the actual supply.

Acknowledgment

The authors thank the Department of Electrical and Electronics Engineering, Stella Mary's College of Engineering, for laboratory facilities and guidance during the project.

References

G. A. Covic and J. T. Boys, "Inductive power transfer," Proceedings of the IEEE, vol. 101, no. 6, pp. 1276-1289, 2013.

J. G. Bolger, F. A. Kirsten, and L. S. Ng, "Inductive power coupling for an electric highway system," in Proc. IEEE Vehicular Technology Conference, 1978.

S. Lee et al., "On-line electric vehicle using inductive power transfer system," in Proc. IEEE Energy Conversion Congress and Exposition.

M. Budhia, J. T. Boys, G. A. Covic, and C.-Y. Huang, "Development of a single-sided flux magnetic coupler for electric vehicle IPT charging systems," IEEE Transactions on Industrial Electronics, vol. 60, no. 1, pp. 318-328, 2013.

A. Rahman et al., "In-vehicle signal information systems and driver behaviour," Transportation Research Part F, 2016.

Arduino, "Arduino Uno documentation," vendor documentation.

SAE International, SAE J2954: Wireless Power Transfer for Light-Duty Plug-in/Electric Vehicles and Alignment Methodology, Recommended Practice, October 2020; revised August 2024. Available: https://www.sae.org/standards/

KAIST, "KAIST's wireless On-Line Electric Vehicle (OLEV) runs inner city roads," KAIST News Centre, August 2013. Available: https://news.kaist.ac.kr/newsen/

Oak Ridge National Laboratory, "ORNL surges forward with 20-kilowatt wireless charging for vehicles," news release, 31 March 2016. Available: https://www.ornl.gov/news/ornl-surges-forward-20-kilowatt-wireless-charging-vehicles

Oak Ridge National Laboratory, "ORNL demonstrates 120-kilowatt wireless charging for vehicles," news release, 19 October 2018. Available: https://www.ornl.gov/news/ornl-demonstrates-120-kilowatt-wireless-charging-vehicles

Oak Ridge National Laboratory, "Polyphase wireless power transfer system achieves 270-kilowatt charge, sets another world record for electric light-duty passenger vehicles," news release, June 2024. Available: https://www.ornl.gov/news/

Michigan Department of Transportation and Electreon, Detroit 14th Street inductive vehicle charging pilot, public project reporting, 2023-2024.

Arena of the Future project (Electreon, Stellantis, A35 Brebemi and partners), 1050 m inductive test track, Chiari, Brescia, Italy, public project reporting, 2022.

VINCI Autoroutes, Electreon, VINCI Construction, Gustave Eiffel University and Hutchinson, "Charge as you drive" dynamic induction charging trial on the A10 motorway, press release, October 2025.